A Protocol for Coupling Volumetrically Dynamic In vitro Experiments to Numerical Physiology Simulation for A Hybrid Cardiovascular Model

Abraham Umo, and Ethan O. Kung

***Abstract*— *Objective:* The Physiology Simulation Coupled Experiment (PSCOPE) is a hybrid modeling framework that enables a physical fluid experiment to operate in the context of a closed-loop computational simulation of cardiovascular physiology. Previous PSCOPE methods coupled rigid experiments to a lumped parameter network (LPN) of physiology but are incompatible with volumetrically dynamic experiments where fluid volume varies periodically. We address this limitation by introducing a method capable of coupling rigid, multi-branch, and volumetrically dynamic in-vitro experiments to an LPN. *Methods:* Our proposed method utilizes an iterative weighted-averaging algorithm to identify the unique solution waveforms for a given PSCOPE model. We confirm the accuracy of these PSCOPE solutions by integrating mathematical surrogates of in vitro experiments directly into the LPN to derive reference solutions, which serve as the gold standard to validate the solutions obtained from using our proposed method to couple the same mathematical surrogates to the LPN. Finally, we illustrate a practical application of our PSCOPE method by coupling an in-vitro renal circulation experiment to the LPN. *Results:* Compared to the reference solution, the normalized root mean square error of the flow and pressure waveforms were 0.001%~0.55%, demonstrating the accuracy of the coupling method. *Conclusion:* We successfully coupled the in-vitro experiment to the LPN, demonstrating the real-world performance within the constraints of sensor and actuation limitations in the physical experiment. *Significance:* This study introduces a PSCOPE method that can be used to investigate medical devices and anatomies that exhibit periodic volume changes, expanding the utility of the hybrid framework.**

***Index Terms*— Hardware in the loop, hybrid model, lumped-parameter network, PSCOPE, mock circuit**

I. Introduction

THE cardiovascular system has conventionally been modeled numerically or experimentally. Numerical simulations such as Lumped parameter network (LPN), finite element models, and multiscale models have been widely used to investigate various hemodynamic parameters; and in-vitro mock circulatory loops have been developed to directly test medical devices and physically model fluid interactions in the cardiovascular system [1-4]. Despite continuous advancements in these approaches, numerical simulations struggle to simultaneously capture mechanics that occur on drastically different time scales — for example, the blade-blood interactions of a rotary blood pump and physiologic responses [5]—[6]; while analogous in-vitro models struggle to accurately reproduce the closed-loop cardiac response of the cardiovascular system [7]—[12]. These respective limitations have motivated the development of hybrid mock circulatory loops which integrate numerical and experimental methods into a single framework, capitalizing on each approach's respective advantages [13]-[17]. These previous implementations demonstrated the potential of using the hybrid approach to investigate the feedback response of the cardiovascular system to dynamic conditions modeled within the framework. However, the real-time feedback required at the experimental-numerical interface has limited such investigations to scenarios that can tolerate significant sensor and actuation limitations. These scenarios typically localize the experimental-numerical interface to the ventricular region of the cardiovascular system where the hemodynamic signals are large and can tolerate measurement and actuation imprecision and delays.

The limitations of prior hybrid mock circulatory loops motivated the development of the Physiology Simulation Coupled Experiment (PSCOPE) [18] which is a hybrid framework that does not require real-time feedback at the experimental-numerical interface. In our previous study we validated the PSCOPE framework against an established multiscale computational fluid dynamics model in the clinical context of a Fontan graft obstruction; we then illustrated the capability of PSCOPE to overcome the limitations of the multiscale computational model by using the hybrid framework to construct a representative scenario of a Jarvik 2000 blood pump implementation for cavopulmonary support in a single-ventricle circulation [18]. This highlights the utility of PSCOPE in modeling the closed-loop physiologic response to blood flow through complex moving geometries of a medical device in operation.

This work was supported in part by Clemson University, an award from the American Heart association and The Children's Heart Foundation under Grant 16SDG29850012 and in part by an award from the National Science Foundation under Grant 1749017.

Abraham Umo is with Clemson University, Clemson, SC, USA. Ethan O. Kung is with Clemson University, Clemson, SC, USA (Corresponding author: Ethan O. Kung; Correspondence e-mail: ekung@clemson.edu).

The main limitation in previous PSCOPE implementations is the inability to couple experiments that exhibit changes in fluid volume. In each PSCOPE model, a coupling protocol directs the exchange of hemodynamic information between the experimental and numerical domains within the hybrid framework. The protocol consists of an algorithm that generates flow rate or pressure boundary conditions for each domain and an operation to iteratively converge the flow and pressure to the model solution. Previously developed proportional-control [18] and Broyden-method [19] algorithms coupled numerical simulations to rigid (either single inlet/outlet or multibranch) experiments but were unable to couple volumetrically dynamic experiments which exhibit periodic changes in fluid volume. Fluid volume in such experiments typically changes due to the compliance of the system enabling the fluid to be stored and released periodically in the experiment.

In this study, we augment the previous PSCOPE coupling methods by presenting an iterative protocol capable of coupling the full range of in-vitro experiments (including volumetrically dynamic, rigid, and multi-branch) to a lumped parameter network (LPN) model of the cardiovascular system. We also investigate factors that impact the convergence efficiency of the coupling operation and offer recommendations for optimizing the process.

II. METHODS

A. Coupling Principle

To illustrate the PSCOPE coupling principle, consider a generic 2-branch (one inlet, one outlet) experimental domain coupled to a generic numerical domain (Fig. 1). The inlet branch of one domain directly interfaces with the outlet branch of the other domain at a junction we refer to as a "coupling junction". In Fig. 1, $P_{subscript}$ and $Q_{subscript}$ correspond to pressure and volumetric flow rate waveforms at the respective branches of each domain. At each coupling junction, there exists a unique flow rate waveform that when applied to both domains (i.e., $Q_{out,num} = Q_{in,exp}$ and $Q_{out,exp} = Q_{in,num}$), would produce the same pressure waveform in both domains (i.e. $P_{out,num} = P_{in,exp}$ and $P_{out,exp} = P_{in,num}$). This set of unique flow rates and corresponding pressure waveforms are collectively referred to as the coupling solution. The goal of our coupling protocol is to identify these solution waveforms by iteratively prescribing boundary conditions (flow rate or pressure waveforms) to each coupling junction and analyzing the resulting flow rate and pressure waveforms. The protocol quantifies the difference (coupling residual) between corresponding experimental and numerical waveforms at each coupling junction and generates new boundary conditions to minimize these residuals, thus identifying the coupling solution.

B. Description of the Coupling Protocol

We designed a coupling protocol to derive the coupling solution via two alternative configurations for any given PSCOPE model where "domain A" corresponds to either the physical or the numerical domain (Fig. 2). For each model

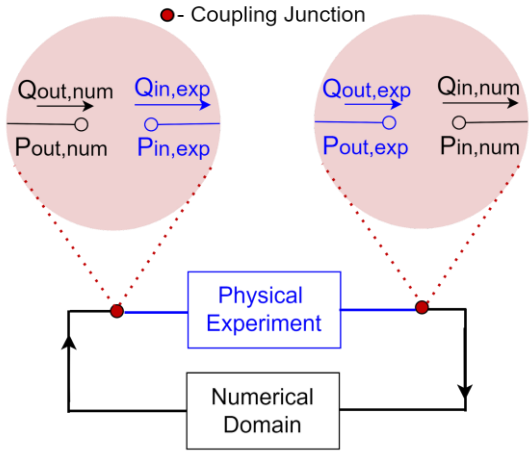

Fig. 1. Schematic of a generic PSCOPE model. P and Q represent pressure and volumetric flow rate waveforms, respectively. Subscripts "in/out; exp/num" represent inlet/outlet locations of experimental/numerical domains.

scenario, the user can select the suitable configuration based on their PSCOPE application and technical preference. Regardless of the configuration implemented, the user initializes the coupling protocol at each coupling junction by prescribing periodic flow rate boundary conditions to domain A and deriving the resulting pressure waveforms. The selected configuration determines if these pressure values are computed or experimentally measured. Subsequently, the user prescribes the derived pressure values as periodic boundary conditions to domain B to obtain the resulting set of flow rate waveforms at each coupling junction. Similarly, the selected configuration determines if these flow rate values are computed or experimentally measured. This process implies that at each coupling junction the pressure waveforms for both domains are identical, but the flow waveforms would differ before the model solution is identified. We will refer to these flow rate waveforms as "coupling flows". For each iteration of the coupling protocol, an algorithm computes a coupling residual via (1) to quantify the difference between coupling flows. The exact coupling solution would result in a coupling residual of 0% Normalized root mean square error (NRMSE) at each coupling junction. In practice, experimental noise introduces a finite residual that limits the protocol to an approximation of the coupling solution. Iterative improvement of this approximation is a tradeoff between the protocol's run time and the accuracy of the derived solution waveforms. Users can balance this tradeoff by specifying an NRMSE threshold as the convergence target. To generate an updated set of flow rate boundary conditions, our algorithm calculates a weighted average of coupling flows via (2). The user then prescribes this new set of flow rate boundary conditions to domain A at their respective coupling junctions to initialize the subsequent iteration of the protocol. Once the convergence target is achieved, we perform one final update of the flow waveforms for each coupling junction via (2) with the "K" coefficients equal to 0.5. This set of resulting flow and pressure waveforms is the coupling solution.

Mass conservation requires the maintenance of the total amount of fluid in a PSCOPE model between iterations. Fluid volume is stored in each domain in capacitors and other fluid

chambers such as those representing the heart. The pressure boundary conditions prescribed to domain B can cause its stored fluid volume to change between the initial and equilibrium states of an iteration, indicating a volume transfer between the domains. Note that this change in volume does not occur in domain A because we always prescribe inflow and outflow rates that have the same average value. For the following iteration, the user adjusts the initial fluid volumes in each domain to reflect the volume transfer indicated by domain B. The volume adjustment must ensure that each iteration begins with the same total volume within the PSCOPE model. As the pressure boundary conditions iteratively converge onto the coupling solution, fluid volume transferred between domains approaches zero. Depending on the sensitivity of a PSCOPE implementation, volume adjustment in each single iteration that is large (compared to the total volume) can hinder convergence, and in some cases lead to runaway divergence of the coupling flows. In such cases, the user should re-run the coupling protocol iteration while applying a fractional scaling factor to the volume adjustment magnitude. In other words, the user updates the volume in both domains to reflect a scaled-down volume transfer between domains, while maintaining a constant total volume. Progressively smaller fractional values may need to be tested until a scaling factor that mitigates divergence in the algorithm's operation is identified.

For $j = 1{:}2$

$$\%\mathrm{NRMSE}(x(j), y(j)) = \frac{\sqrt{\frac{\sum_{i=1}^{N} (x_i(j) - y_i(j))^2}{N}}}{\overline{x(j)}} * 100$$

where: $\begin{bmatrix} x(1) \\ x(2) \end{bmatrix} = \begin{bmatrix} Coupling\ flows\ (Domain\ A) \\ Reference\ Solution\ waveforms \end{bmatrix}$

$$\begin{bmatrix} y(1) \\ y(2) \end{bmatrix} = \begin{bmatrix} Coupling\ flows\ (Domain\ B) \\ Coupling\ Solution\ waveforms \end{bmatrix}$$

$$\begin{bmatrix} Coupling\ Residual \\ Validation\ Residual \end{bmatrix} = \begin{bmatrix} \%NRMSE(x(1), y(1)) \\ \%NRMSE(x(2), y(2)) \end{bmatrix}$$

$\{Subscript\ i\} = Time\ step\ in\ waveform$
$\{N\} = Number\ of\ data\ points\ in\ waveform$
$\{\overline{x(j)}\} = mean\ of\ x(j)$ (1)

$$Q_{n+1} = (K_{Exp} * Q_{Exp,n}) + (K_{Num} * Q_{Num,n})$$

where: $\{Subscript\ Exp, Num\} = Experimental\ and\ Numerical\ domains$
$\{Subscript\ n\} = nth\ iteration$
$\{Q\} = Coupling\ Flows$
$\{K_{Exp}; K_{Num}\} = weighted\ average\ coefficients\ for\ domains;$
$K_{Exp} + K_{Num} = 1$ (2)

C. Preconditioning Protocol

The preconditioning protocol is an optional step to include as needed for specific PSCOPE cases. The flow rate waveforms prescribed to initialize the first iteration of the coupling protocol can impact the ability of the algorithm to converge onto the coupling solution. When these waveforms are very different from those of the coupling solution it can lead the algorithm to diverge with subsequent iterations. This presents a challenge in cases where a reasonable estimation of the coupling solution flow waveforms cannot be obtained. To promote convergence in such cases we present a preconditioning protocol (Fig. 2A) that utilizes a similar iterative procedure as the coupling protocol to first identify steady flow rates that can be used to initialize the coupling protocol and enhance convergence in instances where the algorithm is otherwise diverging. These steady flow rates identified by the preconditioning protocol approximate the cycle-averaged flow waveforms of the coupling solution at each coupling junction. Cycle-averaging is a transformation process that converts a flow rate waveform to a steady flow rate (Fig. 2B). The difference between the preconditioning and coupling protocols is that the former always initializes each iteration with steady flow boundary conditions prescribed to domain A; this involves cycle-averaging the derived flow waveforms from domain B (which may no longer be steady) to generate steady flow rates for the subsequent iteration. The preconditioning protocol iteratively converges the coupling residual between these steady coupling flows below a specified convergence target.

D. Algorithm Testing Using Virtual Experiments

We coupled virtual experiments of different types to LPNs in order to verify the accuracy of the coupling solutions identified by the algorithm [20]. A virtual experiment is a mathematical surrogate that approximates the behavior of a physical experiment and can be either integrated directly into the physiology simulation to constitute a homogeneous model or coupled to the physiology simulation using the PSCOPE framework. Both methods should produce identical solutions albeit through different approaches. The homogenous model produces the reference solution we can use to validate the coupling solution derived from its PSCOPE counterpart.

To this end, we developed two virtual experiments to examine the applicability of the algorithm in modeling fluid systems that exhibit multi-branched flows, mechanically actuated flows, flows through compliant conduits, and discontinuous flows. The closed-loop Fontan circulation LPN model developed by Kung et al. [21] serves as the physiology simulation for demonstrating the operation of the coupling algorithm with these virtual experiments (Fig. 3A).

While theoretically one would not expect the applicability of the coupling algorithm to be dependent on the use of any specific LPN, we include additional data in the supplemental materials to confirm the applicability of the coupling algorithm to a bi-ventricular LPN.

1) Stenotic Pulmonary Circulation Virtual Experiment

The first virtual experiment characterizes the resistance, compliance, and multi-branched features of pulmonary circulation (Fig. 3B). The experiment models vascular stenosis in one of its pulmonary arteries as a quadratic function of flow rate [18], [19], [22] and its parameter values [19], [21] replicate physiologically realistic pressure drops according to prescribed flow rates (Table I). We examined the combined effect of varying protocol configuration and interfacing resistance distribution on the convergence rate of this coupling

operation. Interfacing resistances refer to resistances in each of the PSCOPE domains that are directly adjacent to a coupling junction. To study this effect, we specify a constant pulmonary

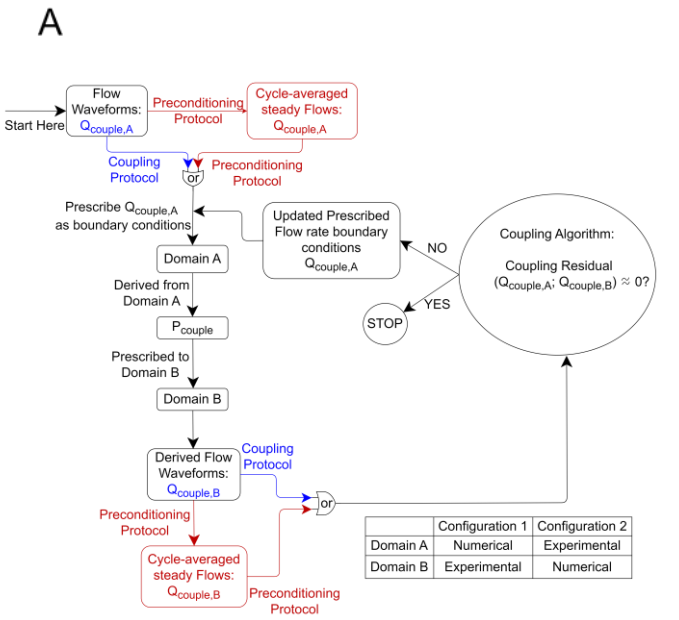

Fig. 2. (A) Flowchart illustration of coupling and preconditioning protocols. The protocol in operation determines the input into "or" gates. $Q_{couple,(A;B)}$ represents coupling flows and P_{couple} represents the set of pressure waveforms shared by both domains at each coupling junction. (B) Illustration of cycle-averaging. Flow rate Waveform (Q) is cycle-averaged to produce a steady flow rate ($Q_{cycle-average}$) based on the mean value of Q.

venous resistance, "R_{pv}", and vary interfacing venous resistances, "$R_{pv,exp}$ & $R_{pv,num}$" as per (3), while coupling the virtual experiment to the LPN using both configurations of the protocol. We applied the preconditioning protocol for the configuration with the virtual experiment being domain A (as it was necessary to avoid divergence); and directly applied the coupling protocol for the alternative configuration. We used physiologically realistic steady flow rates [21] as the initial guess for both.

$$R_{pv} = R_{pv,exp} + R_{pv,num}$$
$$\text{for:} \quad \{R_{pv}\} = 0.0893670\ mmHg\ s\ ml^{-1}$$
$$\left\{\frac{R_{pv,exp}}{R_{pv}}\right\} = [0.125;\ 0.25;\ 0.375;\ 0.5;\ 0.625;\ 0.75;\ 0.875] \quad (3)$$

TABLE I
PARAMETER VALUES FOR VIRTUAL EXPERIMENTS. R- LINEAR RESISTANCE; C-CAPACITANCE; L-INDUCTANCE; K- QUADRATIC RESISTANCE.

Virtual Experiment	R (*mmHg s ml^{-1}*)	C (*ml mmHg^{-1}*)	L (*mmHg s^2 ml^{-1}*)	K (*mmHg s^2 ml^{-2}*)
Stenotic Pulmonary Circulation	R_{pa}= 0.0179 0 < $R_{pv,exp}$ < 0.0894	C_1= 2.32 C_2= 2.32	----------	k = 0.0004
Ventricular Assist Device (VAD)	---------	----------	$L_{VAD,in}$= 1.70 $L_{VAD,out}$= 0.760	$K_{VAD,in}$ = 0.500 $K_{VAD,out}$ = 0.450

2) Berlin Heart Ventricular Assist Device (VAD) Virtual Experiment

We used a computational model characterizing the Berlin Heart Excor device from our previous work [23] as a virtual experiment in this study (Fig. 3C and Table 1). The VAD model simulates the mechanical actuation and discontinuous flow properties observed in the physical device. We initialized the coupling protocol with steady zero value flow rates prescribed as boundary conditions and the VAD model implemented as domain B.

We specified a 1%NRMSE convergence target for both PSCOPE models and evaluated the validation residuals via (1) to quantify the difference between the respective coupling and reference solutions.

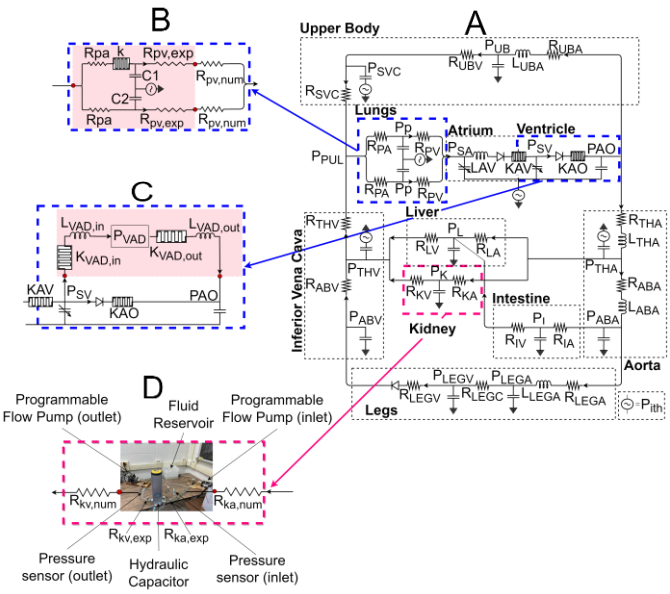

Fig. 3. Illustration of Coupling the Fontan LPN (A) to the virtual stenotic pulmonary circulation (B), virtual VAD (C), and in-vitro Renal circulation experiments (D)

E. Renal Circulation Physical Experiment

We demonstrate the real-world applicability of our coupling algorithm by coupling an in-vitro experiment modeling renal circulation to the LPN (Fig. 3D). The in-vitro model is a resistance-capacitance-resistance (R-C-R) module that mimics the vascular impedance of the kidneys via hydraulic capacitance and resistances. We used an air-pocket based hydraulic capacitor [24] and clamped-flow tubing resistances. The flow circuit consists of the R-C-R module connected in series with programmable flow pumps [25] and a fluid reservoir (Fig. 4). The operating fluid for the experiment is a 40% glycerol solution with a density (1092 kg m^{-3}) and dynamic viscosity (41 x 10^{-4} Pa s) similar to that of human blood [19]. We implemented the in-vitro model as domain A and initialized the preconditioning protocol with physiologically realistic steady flow rate boundary conditions [21] prescribed via programmable flow pumps [25]. We measured the prescribed flow rates via flow modules (TS410 transonic system) connected to flow sensors (16PXL transonic systems; 12PXL transonic systems) and the resulting pressure values via control units (PCU 2000, Millar Instruments) connected to pressure sensors (Model DT-XX, Argon Medical Devices). We acquired all in-vitro measurements via a NI USB-6002 device (DAQ). We used a custom MATLAB program (MATLAB 2019a, The MathWorks, Inc., Natick, Massachusetts, United States) consisting of the coupling algorithm, a program to generate control signals used to manage the operation of the flow pumps, and a low-pass filter (set at 10Hz) to improve experimental signal-to-noise ratio. We ran the physical experiment until periodicity was achieved and used the last cycle of recorded data for analysis. We set the convergence target for this real-world PSCOPE test to be 5% NRMSE.

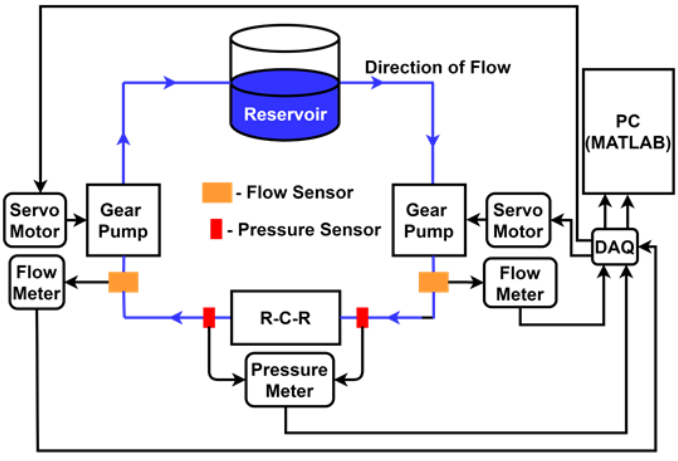

Fig. 4. Schematic of the physical experiment setup

III. RESULTS

A. Algorithm Testing Using Virtual Experiments

The virtual VAD PSCOPE model converged in 9 iterations while the virtual stenotic pulmonary circulation PSCOPE model converged within 47 to 247 iterations, depending on the

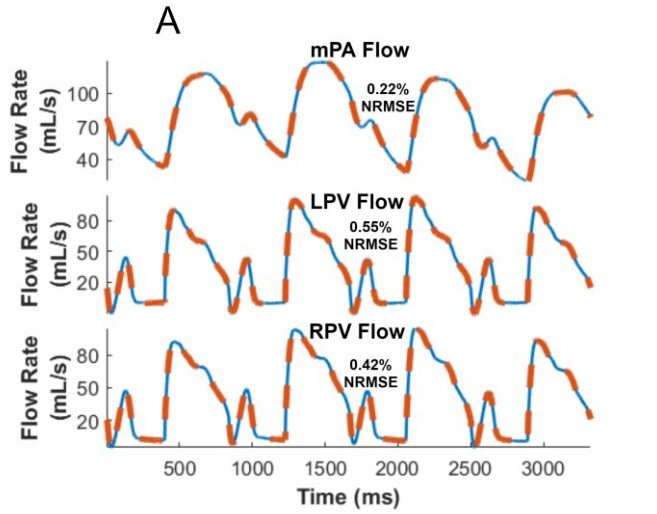

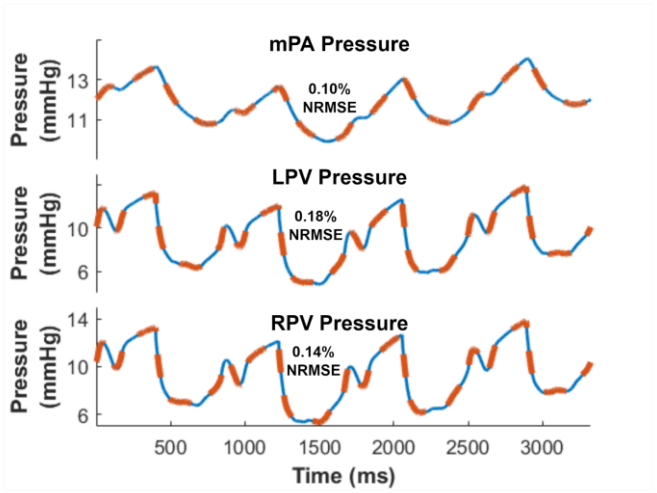

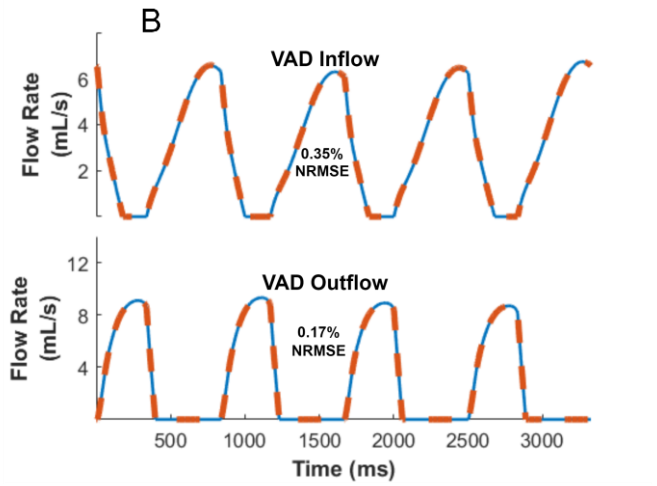

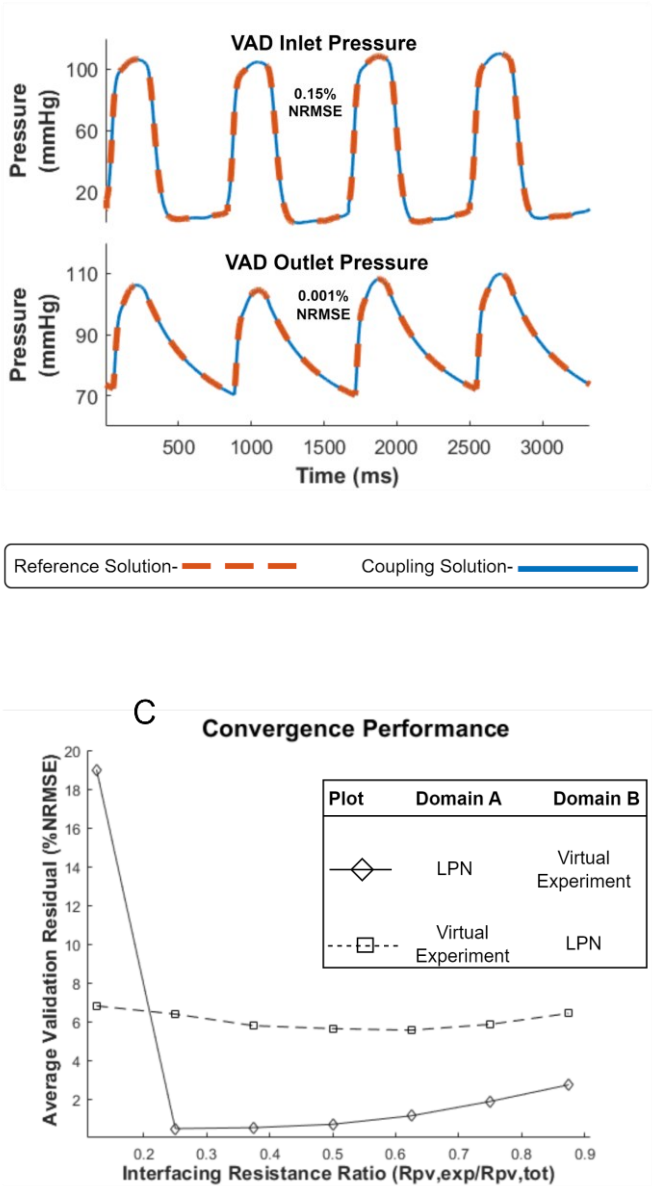

Fig. 5. Comparing coupling and reference solutions for the stenotic pulmonary circulation (A) and VAD (B) virtual experiments. mPA- Main Pulmonary artery; LPV-Left pulmonary vein; RPV- Right pulmonary vein. For (A) the results shown correspond to the case where the interfacing resistance ratio $R_{pv,exp}/R_{pv}$ = 0.5. (C) Convergence rate of the virtual stenotic pulmonary circulation PSCOPE model is quantified by the average validation residual of flow rate waveforms at the 40th iteration.

various implementations of interfacing resistance distribution and protocol configuration selection. For all models involving virtual experiments, the converged validation residuals ranged from 0.001% to 0.55%, confirming the ability of the coupling algorithm to obtain accurate solutions (Fig. 5A and 5B).

We assessed the convergence rate of the stenotic pulmonary circulation PSCOPE model with varying interfacing resistance distributions by examining the pre-converged validation residual of flow rate waveforms at the 40th iteration averaged across coupling junctions. The convergence rate varied across interfacing resistance distributions for both configurations of the coupling protocol (Fig. 5C). Implementing the LPN as domain A resulted in faster convergence rates for all interfacing resistance distributions except one. The optimal convergence rate from implementing the virtual stenotic pulmonary circulation experiment as domain A and B in the protocol occurred at $R_{pv,exp}/R_{pv}$ = 0.625 and $R_{pv,exp}/R_{pv}$ = 0.25 respectively, while the worst convergence rate occurred at $R_{pv,exp}/R_{pv}$ = 0.125 (lowest $R_{pv,exp}/R_{pv}$ value among tested) for both configurations of the protocol.

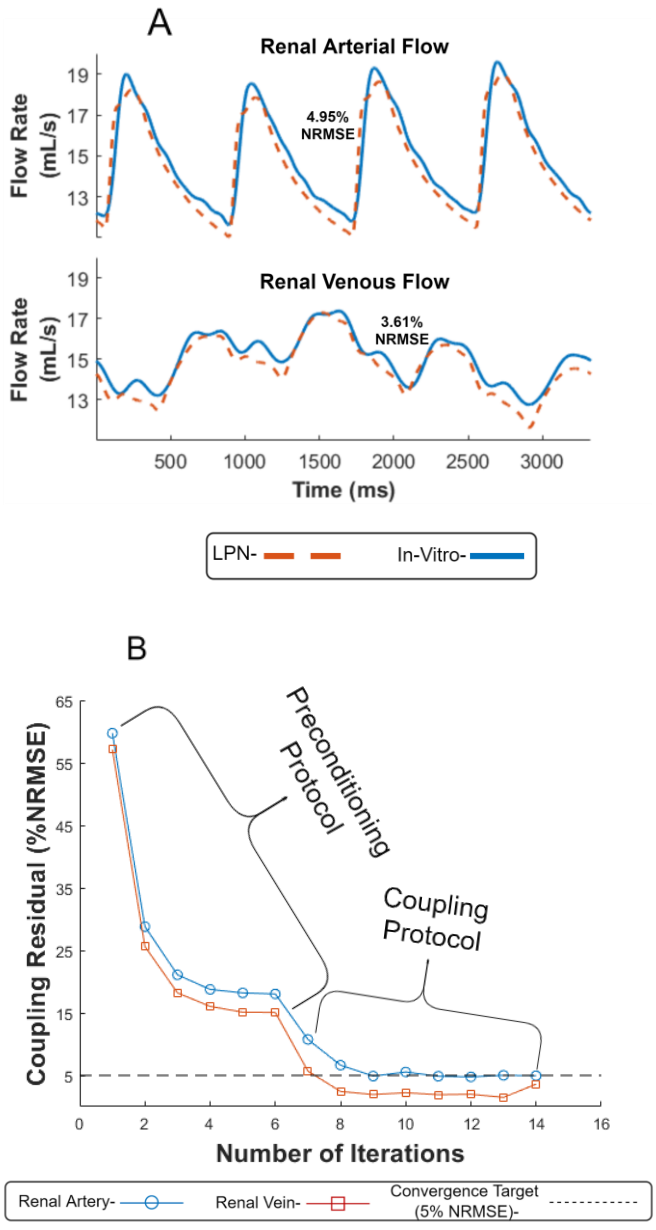

Fig. 6. (A) Coupling Flow waveforms at the 14th iteration of the in-vitro Renal circulation PSCOPE model; (B) Convergence trend of renal coupling flow waveforms. The preconditioning and coupling protocols were executed in iterations 1-6 and 7-14 respectively.

B. Renal Circulation Physical Experiment

The coupling flow waveforms obtained from the in-vitro renal circulation PSCOPE model converged below the 5%

NRMSE convergence target after 9 iterations (Fig. 6). The preconditioning and coupling protocols were executed in iterations 1-6 and 7-14 respectively. The coupling solution was identified at the 9th iteration, but subsequent iterations were continued to confirm the stabilization of the coupling residual. Each iteration required 3 to 5 minutes for execution, resulting in an overall experimental run time of approximately 60 minutes for the entire PSCOPE process.

IV. Discussions

Previous Coupling methods applied identical flow boundary conditions to both PSCOPE domains, and attempt to minimize the residual between the resulting pressure waveforms by iteratively updating the flow waveform prescription [18]—[19]; this approach computes the updated flow waveforms at each time step based on the residual between the resulting pressure waveforms at the same time step, such that for waveforms with N discrete time points these algorithms solve N distinct optimization equations (Fig. 7). Such an approach requires the flow and pressure waveforms to be in phase and is therefore incompatible with volumetrically dynamic experiments where there may be a phase shift between flow and pressure. The coupling method presented in this study does not compute waveform updates via a method that relates pressure and flow at the same time point; our protocol captures phase shifts between flow and pressure when they are sequentially prescribed to each domain within one single iteration, and therefore is compatible with volumetrically dynamic experiments.

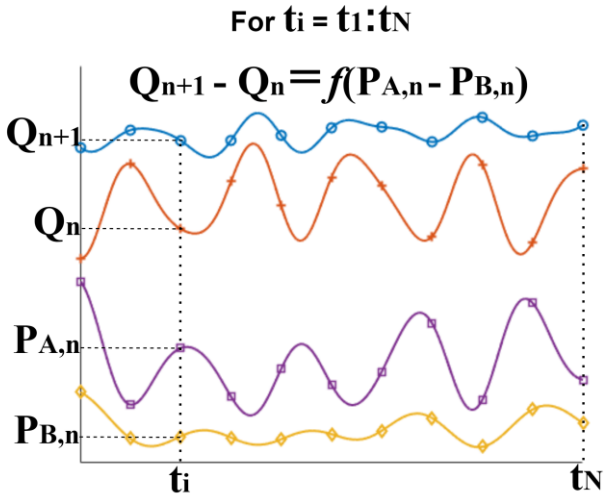

Fig. 7. Illustration of previous coupling approaches which compute the updated flow based on pressure residual at the same time point. N- number of time points in each cycle; t_i- arbitrary time step in the waveform cycle; $P_{(A;B),n}$- pressure values for Domain (A;B) at the nth iteration; $Q_{(n;n+1)}$- flow rate prescriptions for the (n;n+1th) iteration.

Like all optimization problems, the initial flow rate values impact the likelihood and rate of convergence for a PSCOPE implementation. The further these initial values are from the coupling solution the more iterations are required to achieve convergence [19], [26]—[28]. The preconditioning protocol presented in this paper provides users with a standardized approach to obtain initial flow rate values for the coupling protocol. Users can derive a steady flow rate that approximates the cycle-average of the coupling solution flow rate waveforms. This approach offers a high likelihood of convergence and is particularly useful in applications where the algorithm is otherwise diverging.

Protocol configuration is another factor to consider when attempting to optimize the convergence rate of a coupling operation. Alternating between configurations can result in different convergence rates for the same PSCOPE model. For example, we observe worse convergence rates when the LPN is specified as domain B for the model corresponding to Fig. 5C; this is because the pressure boundary condition prescribed to the LPN interferes with the calculated atrial pressure values in the LPN.

We tested the performance of the algorithm with volumetrically dynamic virtual experiments that exhibit multi-branched, mechanically actuated, compliant, and discontinuous flow properties. These virtual experiments can directly integrate with the LPN to result in a homogenous, purely computational model which provides the true solution of the analogous PSCOPE models. The validation residual between the PSCOPE and true solutions quantify the accuracy of the solution identified by the algorithm (Fig. 5A and 5B). We expect the validation residual to be proportional to the coupling residual because we hypothesize that the coupling residual reflects the hybrid model's solution accuracy. In the real-world application of PSCOPE, only the coupling residual is available and thus it is important to confirm that a low coupling residual corresponds to a low validation residual.

Lastly, we demonstrated the real-world applicability and performance of the coupling protocol by coupling an in-vitro experiment containing a compliance chamber to the LPN. The efficient convergence of the coupling flows illustrates the algorithm's robust ability to achieve a reliable approximation of the coupling solution despite the presence of measurement and actuation noises, and other hardware limitations.

Limitations

The coupling protocol presented in this study requires users to prescribe pressure versus flow rate boundary conditions to each PSCOPE domain and cannot be operated in cases where both domains are only compatible with the same type of boundary condition. The technical feasibility of prescribing flow rate or pressure waveforms to each branch of a PSCOPE domain determines its compatibility with each type of boundary condition. For instance, there are currently no commercially available devices for prescribing pressure boundary conditions to a physical experiment, and various locations in an LPN have limitations regarding flow rate or pressure prescriptions. Further research is required to develop a protocol to tackle these scenarios. Finally, the zero-dimensional nature of the LPN makes it unsuitable for investigations of phenomena that include spatial dimensions in the analysis (i.e. wave reflections, etc); therefore, with the particular setup presented in this study, the user must investigate those phenomena by including the relevant

segments in the experimental domain. If there is a need to model spatial phenomena computationally in a hybrid model, future research is needed to confirm the coupling performance when the computational domain consists of a reduced-order model (such as a 1-D model) that is capable of modeling spatial effects.

V. CONCLUSION

The PSCOPE model is a closed-loop hybrid framework capable of capturing the dynamic response of a simulated cardiovascular system to various flow and fluid-structure interactions modeled experimentally. In this study, we present a protocol capable of coupling volumetrically dynamic in-vitro experiments to an LPN physiology simulation, overcoming the limitations of previous PSCOPE coupling methods. The coupling protocol enables the exchange of pressure and flow rate information between each of the PSCOPE domains by employing an iterative weighted averaging algorithm to identify the coupling solution. The results from comparing the reference and coupling solutions of PSCOPE models containing virtual experiments confirm the ability of the algorithm to identify accurate solutions. We also recognize the significance of the initial flow rate values in affecting convergence and described a preconditioning procedure to obtain a steady flow rate value that mitigates divergence. Furthermore, we show that other factors such as protocol configuration and interface resistance distribution can impact convergence efficiency in each application. Finally, the algorithm successfully coupled an in-vitro renal circulation physical experiment to the LPN, demonstrating its potential for real-world applications such as medical device testing and disease state modeling.

DATA AVAILABILITY

The source code for the virtual PSCOPE and integrated model simulations in this study are openly available in Zenodo at https://doi.org/10.5281/zenodo.7154220, reference [20].

How to Cite This Paper

Umo A, Kung E. "A Protocol for Coupling Volumetrically Dynamic In vitro Experiments to Numerical Physiology Simulation for A Hybrid Cardiovascular Model" ***IEEE Transactions on Biomedical Engineering.*** **DOI: 10.1109/TBME.2022.3216542 (2022)**

REFERENCES

[1] Kung EO, et al. In vitro validation of finite-element model of AAA Hemodynamics incorporating realistic outlet boundary conditions. J Biomech Eng. 2011;133(4):041003. https://doi.org/10.1115/1.4003526

[2] Taylor CA, Draney MT. Experimental and computational methods in cardiovascular fluid mechanics. Annu Rev Fluid Mech. 2004;36(1):197-231. https://doi.org/10.1146/annurev.fluid.36.050802.121944

[3] Cebral JR, et al. Characterization of cerebral aneurysms for assessing risk of rupture by using patient-specific computational hemodynamics models. Am J Neuroradiol. 2005;26(10):2550-2559. https://doi.org/10.1016/S0098-1672(08)70473-9

[4] Kung EO, et al. In vitro validation of finite element analysis of blood flow in deformable models. Ann Biomed Eng.2011;39(7):1947-1960. https://doi.org/10.1007/s10439-011-0284-7

[5] Jing T, Cheng Y, Wang F, Bao W, Zhou L. Numerical Investigation of Centrifugal Blood Pump Cavitation Characteristics with Variable Speed. *Processes*. 2020; 8(3):293. https://doi.org/10.3390/pr8030293

[6] Drešar, Primož*; et al. A Numerical Simulation of HeartAssist5 Blood Pump Using an Advanced Turbulence Model. ASAIO Journal: September/October 2018 - Volume 64 - Issue 5 - p 673-679 doi: 10.1097/MAT.0000000000000703

[7] D. L. Timms, et al. "Haemodynamic modeling of the cardiovascular system using mock circulation loops to test cardiovascular devices," *2011 Annual International Conference of the IEEE Engineering in Medicine and Biology Society*, 2011, pp. 4301-4304, doi: 10.1109/IEMBS.2011.6091068.

[8] Gehron, Johannes; et al. For the EMPACS (Exploration of the mixing phenomena during interaction of internal and external circulations) study group. Development and Validation of a Life-Sized Mock Circulatory Loop of the Human Circulation for Fluid-Mechanical Studies. ASAIO Journal: November/December 2019 - Volume 65 - Issue 8 - p 788-797doi: 10.1097/MAT.0000000000000880

[9] Timms, D.L., et al. (2011), A Compact Mock Circulation Loop for the In Vitro Testing of Cardiovascular Devices. Artificial Organs, 35: 384-391. https://doi.org/10.1111/j.1525-1594.2010.01088.x

[10] M. Vilchez-Monge, et al. "Design and construction of a hydro-pneumatic mock circulation loop that emulates the systemic circuit of the circulatory system," *2016 IEEE 36th Central American and Panama Convention (CONCAPAN XXXVI)*, 2016, pp. 1-6, doi: 10.1109/CONCAPAN.2016.7942336.

[11] Franzetti, G., et al. (October 11, 2019). "Design of an In Vitro Mock Circulatory Loop to Reproduce Patient-Specific Vascular Conditions: Toward Precision Medicine." ASME. *ASME J of Medical Diagnostics*. November 2019; 2(4): 041004. https://doi.org/10.1115/1.4044488.

[12] Gregory SD, et al. An advanced mock circulation loop for in vitro cardiovascular device evaluation. Artif Organs. 2020 Jun;44(6):E238-E250. doi: 10.1111/aor.13636. Epub 2020 Feb 3. PMID: 31951020.

[13] Petrou A, et al. Versatile Hybrid Mock Circulation for Hydraulic Investigations of Active and Passive Cardiovascular Implants. ASAIO J. 2019 Jul;65(5):495-502. doi: 10.1097/MAT.0000000000000851. PMID: 30045051; PMCID: PMC6615934.

[14] Rapp ES, et al. Hybrid Mock Circulatory Loop Simulation of Extreme Cardiac Events. IEEE Trans Biomed Eng. 2022 Sep;69(9):2883-2892. doi: 10.1109/TBME.2022.3156963. Epub 2022 Aug 19. PMID: 35254970.

[15] T. Salesch, et al, "Parameter optimization and validation of a cost efficient hybrid mock loop of the cardiovascular system," 2021 European Control Conference (ECC), 2021, pp. 762-768, doi: 10.23919/ECC54610.2021.9654952.

[16] D. Telyshev, et al, "Hybrid mock circulatory loop for training and study purposes," 2018 Ural Symposium on Biomedical Engineering, Radioelectronics and Information Technology (USBEREIT), 2018, pp. 29-32, doi: 10.1109/USBEREIT.2018.8384542.

[17] Korn L, et al. Real-time ecg simulation for hybrid mock circulatory loops. *Artif Organs* 2018; **42**: 131– 40.

[18] Kung. E et al. (2019). A Hybrid Experimental-Computational Modeling Framework For Cardiovascular Device Testing. *Journal of Biomechanical Engineering*. 10.1115/1.4042665.

[19] Mirzaei. E, et al. An algorithm for coupling multibranch in vitro experiment to numerical physiology simulation for a hybrid cardiovascular model. *Int J Numer Meth Biomed Engng*. 2020; 36:e3289. https://doi.org/10.1002/cnm.3289

[20] Umo, Abraham, & Kung, Ethan. (2022). A Protocol for Coupling Volumetrically Dynamic In vitro Experiments to Numerical Physiology Simulation for A Hybrid Cardiovascular Model (Version 1). Zenodo. https://doi.org/10.5281/zenodo.7154220

[21] Kung. E, et al (2014). A simulation protocol for exercise physiology in Fontan patients using a closed loop lumped-

parameter model. *Journal of biomechanical engineering*, *136*(8), 0810071–08100714. doi:10.1115/1.4027271

[22] Ha H, et al. Estimating the irreversible pressure drop across a stenosis by quantifying turbulence production using 4D flow MRI. Sci Rep. 2017;7(2016):1-14. https://doi.org/10.1038/srep4661

[23] Schmidt T, et al. "Superior performance of continuous over pulsatile flow ventricular assist devices in the single ventricle circulation: A computational study." Journal of Biomechanics. 52:48-54 (2017)

[24] Kung E, Taylor C, "Development of a Physical Windkessel Module to Re-Create In Vivo Vascular Flow Impedance for In Vitro Experiments." Cardiovascular Engineering and Technology. s

[25] Mechoor R, et al. "A Real-Time Programmable Pulsatile Flow Pump For In-Vitro Cardiovascular Experimentation." Journal of Biomechanical Engineering. 138(11):111002 (2016)

[26] Dennis JE, Schnabel RB. Numerical Methods for Unconstrained Optimization and Nonlinear Equations. Society for Industrial and Applied Mathematics; 1996.

[27] Martinez JM. Practical quasi-Newton methods for solving nonlinear systems. Journal of Computational and Applied Mathematics 2000; 124(1–2):97–121. doi:10.1016/S0377-0427(00)00434-9.

[28] Nocedal J, Wright SJJ. Numerical Optimization. Springer New York; 2006